New MoO3-CeO2-ZrO2 and WO3-CeO2-ZrO2 nanostructured mesoporous aerogel catalysts for the NH3-SCR of NO from diesel engine exhaust

Jihene Arfaoui, Abdelhamid Ghorbel, Carolina Petitto, Gerard Delahay

New MoO_3-CeO_2-ZrO_2 and WO_3-CeO_2-ZrO_2 nanostructured mesoporous aerogel catalysts for the NH_3-SCR of NO from diesel engine exhaust

Jihene Arfaoui*[a], Abdelhamid Ghorbel[a], Carolina Petitto[b], Gerard Delahay[b]

[a]Université Tunis El Manar, Laboratoire de Chimie des Matériaux et Catalyse, Département de Chimie, Faculté des Sciences de Tunis, Campus Universitaire Farhat Hached d'El Manar, 2092, Tunis, Tunisia.
[b]ICGM, University of Montpellier, ENSCM (MACS), CNRS, Montpellier, France

Abstract

New MoO_3 or WO_3 modified CeO_2-ZrO_2 aerogel catalysts were elaborated using the sol gel method combined to supercritical drying for the NO-SCR by NH_3 in excess of O_2. XRD, N_2-Physisorption, NH_3-TPD, H_2-TPR and DRUV-Vis spectroscopy were used to analyse the samples. The results reveal that all the aerogel powders (ZrO_2, CeO_2-ZrO_2, MoO_3- ZrO_2, WO_3-ZrO_2, MoO_3-CeO_2-ZrO_2 and WO_3-CeO_2-ZrO_2), calcined at 500 °C, are nanostructured and mesoporous materials, developing essentially the diffraction peaks of the ZrO_2 tetragonal phase, which was stabilized by the presence of cerium. Ce, Mo and W species were found highly dispersed on the zirconia surface, their nature and the diverse interactions developed between them affect the crystallites size of ZrO_2, acidity, reducibility, surfaceoxygen mobility of catalysts and influence extremely their SCR activity. Higher NO-SCR performances are obtained, between 200 and 500 °C, over the new ternary MoO_3-CeO_2-ZrO_2 and WO_3-CeO_2 ZrO_2 catalysts compared to corresponding binary systems (CeO_2-ZrO_2, MoO_3-ZrO_2 and WO_3-ZrO_2). This discloses a synergism in the NO-SCR related to the existence of strong interactions Ce↔Mo and Ce↔W. Interestingly, above 90 % NO conversions into essentially N_2 (≥ 97 %) are achieved between 350 and 500 °C over the most efficient MoO_3-CeO_2-ZrO_2 ternary catalyst. Keywords: Sol Gel procedure, New CeO_2-ZrO_2 aerogel catalyst, MoO_3, WO_3, Ce↔Mo and Ce↔W interactions, NO removal from diesel engine exhaust.

1.Introduction

Selective catalytic reduction of nitrogen oxides by ammonia (NO-SCR by NH_3), based on the reaction between NH_3 and NO_x to produce N_2 and H_2O, is considered as one of the most effective technology for the NO_x removal from stationary sources and diesel engine exhausts [1,2]. The current commercial catalysts for this process are V_2O_5-WO_3/TiO_2 and V_2O_5-MoO_3/TiO_2. Unfortunately, the narrow windows of the optimal operation temperature (300-400 °C), formation of N_2O at high temperature and toxicity of vanadium restrained the practical applications of V-based catalysts for diesel vehicles [2,3]. Therefore, there are continuing efforts to develop new free vanadium SCR catalysts for the control of NO_x emissions from diesel engines. Cerium, as a rare earth metal, has been proved to be very active in catalysing NO reduction by NH_3 due to its unique oxygen storage capacity (OSC), redox and acid-base properties [4]. However, the low thermal stability and the susceptibility to be sintered at high temperature remain the major drawbacks of pure CeO_2 [5]. To overcome this problem, Ce has ofen been supported on many oxides which has leads to highy actives mixed oxides catalysts in the NH_3-SCR reaction, such as : Ce-Ti, Ce-Fe-Ti, Ce-Cu-Ti, Ce-Co-Ti, Ce-Bi-Ti, Ce-Sn-Ti, Ce-W-Ti, Ce-Mo-Ti, Ce-Nb-Ti, Ce-Si-Ti and Ce-Zr-Ti [6,7]. Hori et

al. [8] reported that the OSC and thermal stability of ceria could be improved by adding ZrO_2. Moreover, Li et al. [9] stated that introducing Zr into CeO_2 can generate oxygen vacancies and thus increases the catalytic activity. On the other hand, many studies proved that W-Ce oxides exhibit high catalytic performances in the NH_3-SCR reaction [10-12]. Shan et al. [10] reported that Ce-W mixed oxide catalyst, prepared by homogeneous precipitation method, presented nearly 100 % NO_x conversion in a wide temperature range (250 to 425 °C). The authors [11] concluded also that, $CeWO_x$ catalyst was highly efficient for NO_x removal and could make diesel engine meet the Euro V limit. It was demonstrated that adding WO_3 into CeO_2-based catalysts strengthens their surface acidity and generates more abundant Ce^{3+}, which enhances their SCR activity [13]. Recently, Xu et al. [14], revealed that the presence of WO_3 in Ce-Zr mixed oxides catalysts can inhibit the oxidation of NH_3 and enhances the SCR activity at high temperature. Consequently, WO_3-CeO_2-ZrO_2 catalysts have attracted recently much attention as a potential SCR catalyst for removing NOx emitted from diesel engine [3,9,15-17]. Li et al.[15], showed that a WO_3/CeO_2-ZrO_2 catalyst, prepared by the impregnation method, exhibits high SCR activity in the 300-500 °C temperature range. Meanwhile, Song et al. [3] demonstrated that above 90 % NO conversion was obtained at 201-459 °C, under a gas hourly space velocity (GHSV) of 60 000 h^{-1}, over a CeO_2-ZrO_2-WO_3 catalyst, prepared by the hydrothermal way. Similarly, Li et al. [9] reported that a CeO_2-ZrO_2-WO_3 system, prepared also by the hydrothermal route, yields more than 90% NO conversion in a wide temperature range (250- 500 ºC) using a GHSV of 60 000 h^{-1}. The authors concluded that the high surface area, the strongest synergistic interaction, the superior redox property and the highly dispersed or amorphous WO_3 species contributed to the excellent SCR activity of CeO_2-ZrO_2-WO_3 catalyst. In a recent investigation [18], Liu et al. showed that CeO_2-WO_3-ZrO_2 catalyst, prepared by the homogeneous precipitation method, exhibits excellent NH_3-SCR activity for NOx removal and hydrothermal stability. In fact, 80 % NOx conversion was achieved at 300- 500 °C under a high gas hourly space velocity of 250,000 h-1 over the CeO_2-WO_3-ZrO_2 catalyst after its hydrothermal aging at 850 °C for 16 h. As for WO_3, MoO_3 is widely used as stabilizer and promoter to improve the activity, structural and mechanical properties of V_2O_5/TiO_2 commercial SCR catalysts. Despite the fact that MoO_3-CeO_2/TiO_2 catalysts have been extensively studied and have showed a good NOSCR activity [19-22], only a few papers related to the investigation of MoO_3-CeO_2-ZrO_2 SCR catalysts have been reported in the literature [23,24]. In this framework, novel Mo promoted Ce-Zr mixed oxide catalysts were prepared by homogeneous precipitation method and used for the SCR of NO_x by NH_3 [23]. The results showed that adding Mo inhibits the growth of CeO_2 particle size, improves the redox ability and increases the amount of surface acidity, which leads to the excellent NO-SCR performances observed. In addition, Liu et al. [24] developed, via the hydrothermal-impregnation method, a novel MoO_3/CeO_2-ZrO_2 SCR catalyst and concluded that a synergetic effect between Mo and CeO_2-ZrO_2 contributes to the adsorption and activation of NH_3, thus leading to high catalytic SCR activity between 250 and 400 °C, under a GHSV of 98 000 h^{-1}. Based on the above discussion and motivated by the fact that, until now, any study devoted to the exploration of WCeZr and MoCeZr aerogel systems in the NO-SCR by NH_3 process has not been described in the literature, we have developed in this work, using the one step sol gel method combined to supercritical drying, a new WO_3-CeO_2-ZrO_2 and MoO_3- CeO_2-ZrO_2 aerogel catalysts for DeNOxing in a wide temperature range (150-500 °C) under O_2 rich conditions and at relatively high GHSV (120.000 h^{-1}).

2. Experimental

2. 1. Synthesis of aerogel catalysts

The aerogel samples (ZrO_2, CeO_2-ZrO_2, MoO_3-ZrO_2, WO_3-ZrO_2, MoO_3-CeO_2-ZrO_2 and WO_3-CeO_2-ZrO_2) were synthesized via the one step sol-gel method according to the procedure described in our previous work [25]. So, for the preparation of a desired mass of pure zirconia, a suitable quantity of Zr precursor (Zirconium (IV) butoxide, $Zr(OC_4H_9)_4$, Sigma-aldrich, 80 %) was dissolved, at room temperature and under continuous stirring, in an appropriate volume of anhydrous ethanol (C_2H_6O, Aldrich, 99.8 %) used as a solvant (the molar ratio nEthanol/nZr and the final concentration of ethanol were fixed to 1 and 1M, respectivelly). Then, the needed amount of a complexing agent (Ethyl acetoacetate, $C_6H_{10}O_3$, Fluka, > 99.5%), yielding a molar ratio nEtacac/nZr =1, was introduced into the mixture to control the reactions rate. After 1h, a dilute solution of HNO_3 (0.1 M) was gradually added, with a molar ratio nH^+/nZr = 10, to accomplish hydrolysis, and the slurry was keep under stiring until the gelification. Finally, the resulting gel was transformed into ZrO_2 aerogel powder by drying in an autoclave under the supercritical drying conditions of the ethanol (T = 243 °C and P = 63 bar). All the catalysts were prepared using the same methodology; cerium (III) nitrate hexahydrate ($Ce(NO_3)_3$,6 H_2O, Sigma-aldrich, ≥ 98.5 %), ammonium heptamolybdate hydrate ($(NH_4)_6Mo_7O_{24}.4H_2O$, Sigma Aldrich, > 99.0%) and ammonium metatungustate hydrate ($(NH_4)_6H_2W_{12}O_{24}.xH_2O$, Sigma Aldrich, > 99.9%) were used as Ce, Mo and W sources, respectively. Their calculated amounts, giving a theoretical loadings of 10 % wt. CeO_2, 10 % wt. MoO_3 and 10 % wt. WO_3, were introduced (successively, Ce then Mo/or W) in the slurry and stirred 1h (for each element) before the hydrolysis step (a few quantity of an aqueous solution of $H_2C_2O_4.2H_2O$ (1M) was employed to facilitate the dissolution of Mo and W precursors before use). All the obtained aerogel powder were calcined for 3 h at 500 °C under O_2 flow (30 mL min^{-1}).

2. 2. Characterization of catalysts and SCR activity test

Powder X-ray diffraction patterns of catalysts were recorded, from 2θ = 2 to 80 ° with a step size of 0.02 °, on a Brüker AXS D8 XRD system using CuKα radiation (λ = 1.5406 Å). The crystallites size (D) of ZrO_2 was calculated by the Scherrer formula applied to the most intense peak of the ZrO_2 tetragonal phase (2θ ~30.20 °): $D = 0.89 (\lambda / \beta \cos\theta)$ [26], where θ is the peak position, β is the corrected peak width at half-maximum intensity (FWHM in radians) and λ is the wavelength of XR radiation.

The BET surface area, total pore volume, average pore diameter and pore size distribution of all the aerogel powder were determined by multipoint N_2-adsorptiondesorption method, at liquid N_2 temperature (77 K), using an ASAP 2020 (Micromeritics) instrument. Before measurements, the powder (m = 0. 1 g) was degassed at 200 °C for 6 h to evacuate any adsorbed moisture. The residual pressure reached during the degassing step was 10^{-5} torr. The specific surface areas were calculated by the Brunauer-Emmett-Teller (BET) equation, while, the pore volume, average pore diameter and pore size distribution were determined by Barrett- Joyner-Halenda (BJH) method from the desorption branches of the isotherms.

Diffuse Reflectances Ultraviolet visible spectroscopy (DR-UV-vis) was carried out over the aerogel powders on a lambda 45 PerkinElmer spectrophotometer equipped with an integrating sphere type RSA-PE-20. The UV-vis spectra were acquired between 200 and 900 nm with a speed of 960 nm min^{-1} and an aperture of 4 nm.

Ammonia temperature programmed desorption (NH_3-TPD) experiments were performed in an AUTOCHEM 2920 (Micromeritics) equipped with a TCD detector. Prior to NH_3 adsorption, the catalyst powder (m= 0.05 g), placed in a U-shaped quartz tube, was activated under air flow at 500 °C for 30 min (flow rate = 30 mL min^{-1} and ramp = 10 °C min^{-1}). After cooling to 100 °C, the sample was exposed to 5 vol % NH_3 balanced with He for 45 min (30 mL min^{-1}) to ensure that the adsorption sites were saturated with ammonia. Then, helium (30 mL min^{-1}) was used to purge the catalyst during 2 h for eliminating the weakly

adsorbed NH_3. Finally, the ammonia was desorbed in He (30 mL min^{-1}) from 100 °C to 600 °C at a ramp rate of 10 °C min^{-1}.

Hydrogen temperature programmed reduction (H_2-TPR) analyses were conducted using an AUTOCHEM 2910 (Micromeritics). Firstly, the aerogel powder (m = 0.05 g) was pre-treated with 5 vol % O_2 in He (30 mL min^{-1}) at 500 °C for 30 min (ramp 10 °C min^{-1}). After being cooled down to 50 °C in the same atmosphere, it was flushed with He (30 mL min^{-1}) to purge any weakly chemisorbed oxygen species. The catalyst was then reduced in a flow of 5 vol % H_2 in Ar (30 mL min^{-1}) from 50 to 800 °C (10 °C min^{-1}). At the same time the signal was registered by a thermal conductivity detector.

The selective catalytic reduction of NO by NH_3 (NO-SCR or NH_3-SCR) was realized in a fixed-bed quartz flow reactor operating at atmospheric pressure. The catalyst (0.05 g) was activated in situ at 200 °C for 30 min under O_2/He flow (20/80, v/v) then cooled to 150 °C. A feed gas stream, containing 1000 ppm NO, 1000 ppm NH_3, 8 % O_2 balanced with He and 3.5 % H_2O was supplied through mass flow controllers to the micro-reactor with a total flow rate of 100 cm^3 min^{-1} yielding a gas hourly space velocity (GHSV) of 120,000 h^{-1}. The SCR was carried out on programmed temperature from 150 to 500 °C with the heating rate 6 °C min^{-1}. The reactants and products were continuously analyzed by a quadruple gas mass spectrometer (Pfeiffer Omnistar) equipped with Channeltron and Faraday detectors (0-200 amu).

3. Results and discussion

3. 1. Structural properties of aerogel catalysts

The cristallinity of catalyst, which is obviously affected by the preparation method and calcination treatment, is a major factor influencing its De-NOx behaviour [27,28]. Figure 1 depicts the XRD patterns of powder aerogel catalysts. As it can be seen, the ZrO_2, MoO_3-ZrO_2 and WO_3-ZrO_2 are well structured materials and develop both the diffraction peaks of tetragonal and monoclinic phases of ZrO_2 (labelled as t-ZrO_2 and m-ZrO_2, respectively). Hence, the most intense reflections, observed at $2\theta \approx 30{,}18°$ (hkl:101), 34,89° (002), 50,34° (112), 60,12° (211), 62,86° (202) and 74.60 ° (220), are ascribed to the t-ZrO_2 phase [ICSD #: 066787]. However, those located at $2\theta \approx 24{,}33°$ (110), 28,45° (-111), 40, 78° (-211), 45,26° (-202), 54.04° (202) and 55.64 ° (-113), are attributed to the m-ZrO_2 phase [ICSD #: 089426]. By contrast, only the diffraction peaks corresponding to the tetragonal phase of the zirconia are identified on the diffractogramms of catalysts containing cerium (CeO_2-ZrO_2, MoO_3-CeO_2-ZrO_2 and WO_3-CeO_2-ZrO_2). This proves a stabilization of the tetragonal phase of ZrO_2 by the cerium incorporation. Some investigators have linked this t-ZrO_2 phase stabilization to a particles size effect, with smaller particle size having greater surface energy contribution to their stability [28-31]. Besides, it has been related to the pressure and the presence of phase stabilizers in the bulk, usually as rare earth cationic dopants with intrinsic defects associated with them [28,29]. Gravie [30] reported that the tetragonal phase appeared to be critical crystallites size about 30 nm and above that point the t-ZrO_2 phase could not be stabilized at room temperature. On the other hand, W. Khaodee et al. [31] noticed the disappearance of the monoclinic phase of ZrO_2 after the incorporation of 12.7 wt. % CeO_2. The authors concluded that the addition of CeO_2 into ZrO_2 results in not only the reduction of crystallites size, but also the increase of lattice defects due to replacement of Zr^{4+} with larger cation such as Ce^{4+}.

It should be mentioned that no typical peaks (most intense ones) of CeO_2 ($2\theta = 28.55$ (111), [PDF 00-034-0394]), MoO_3 ($2\theta = 25.80$ (210), [PDF 00-021-0569]) and WO_3 ($2\theta = 23.70$ (110), [ICSD 01-089-8053]) bulk oxides are perceived in the XRD patterns of all the catalysts which reveals the highly dispersion state of cerium, molybdenum and/or tungsten species on the ZrO_2 surface.

Based on the above XRD analysis and taking into account the calculated values of ZrO_2 crystallites size (listed in table 1), it can be confirmed the successful synthesis of new

generation of nanostructured SCR catalysts characterized by a good cristallinity of the zirconia tertragonal phase and constituted by nano-crystallites with a size in the range of 6.6-10.6 nm.

3. 2. Textural properties of aerogel catalysts

The main textural properties of catalysts (specific surface area, pore volume and average pores diameter) are summarized in Table 2. Based on these results, it can be concluded that all the samples calcined at 500 °C exhibit a high surface area ($93 \leq S_{BET} \leq 168$ m^2/g), large porosity ($0.35 \leq V_{PT} \leq 0.55$ cm^3/g) and mesoporous distribution ($77 \leq \Phi_{pore} \leq 111$ Å) reflecting their developed mesoporous texture and good thermal stability. Noting that all the catalysts show a higher surface area ($S_{BET} \geq 130$ cm^3/g) compared to ZrO_2 support (93 cm^3/g). This is due to the decrease of the crystallites size of support after the deposition of Ce, W and Mo active species as revealed in Table 1. It is recognized that large specific surface area implies more active sites exposed on the surface of catalyst and more contact opportunities with gas molecules, which can promote the SCR activity [32].

Figure 2 displays the nitrogen adsorption-desorption isotherms and corresponding pore size distribution curves of samples. It is clearly seen that all the aerogel materials exhibit a type IV isotherm, elucidating their mesoporous texture according to the IUPAC rules [33]. H1 hysteresis loop, in which the adsorption and desorption branches of the isotherm are substantively parallel indicating the presence of cylindrical mesoporous channels [34], is found in the case of ZrO_2, CeO_2-ZrO_2, MoO_3-ZrO_2 and MoO_3-CeO_2-ZrO_2 solids. Nevertheless, WO_3-ZrO_2 and WO_3-CeO_2-ZrO_2 catalysts display a H2 type of hysteresis loop which is linked to inkbottle pores [35]. As shown also in Fig. 2 all the samples are characterized by a unimodal pores distribution .

3. 3. Supported active species characterization

Diffuse reflectance spectroscopy, in the UV-vis range, was aimed to determine the oxidation state and coordination environment of supported actives species (Ce, W and Mo). The results are presented in Fig. 3. In addition, the typical absorption bands characterizing molybdenum and tungsten species and their attributions, according to the literature reports, are given in Table 3. As shown, only one absorption band connected with $O^{2-} \rightarrow Zr^{4+}$ ligand to metal charge transitions ((LMCT), corresponding to the excitation of electron from the valence band having O2p character to the conduction band having Zr3d character, is observed between 200 and 250 nm, in the UV visible spectra of ZrO_2 aerogel support [36-37].

However, additional bands are detected, in the 200-400 nm range, in the case of binary systems. Thus, for CeO_2-ZrO_2, the bands located in the 220-250 and 280-400 nm ranges correspond to $O^{2-} \rightarrow Ce^{3+}$ and $O^{2-} \rightarrow Ce^{4+}$ LMCT, respectively [25]. The bands detected between 200 and 350 nm in the UV-vis spectra of MoO_3-ZrO_2 and WO_3-ZrO_2 can be ascribed to $O^{2-} \rightarrow M^{6+}$ LMCT (M = Mo; W) of (i) highly dispersed isolated M^{6+} species (like WO_4^{2-} and MoO_4^{2-}) in tetrahedral coordination (normally between 200-270) [34,38-43]) and (ii) $O^{2-} \rightarrow M^{6+}$ LMCT (M = Mo; W) of polymeric M^{6+} species in octahedral coordination (polymolybdates and polytungstates, usually in the ranges of 260-280 nm [41,43] and 300-380 nm [34,38-43]). For the ternary catalysts, the largest and more intensive bands (compared to those of corresponding binary; MoO_3-ZrO_2 and WO_3-ZrO_2) detected between 200 and 400 nm can imply the presence of all the former cited species (Ce and Mo for MoO_3-CeO_2-ZrO_2; Ce and W in the case of WO_3-CeO_2-ZrO_2). Markedly, no bands belonging to WO_3 (430-450 nm [41]) and most probably also MoO_3 (> 320 nm [42]) crystalline phases are found for all the catalysts demonstrating, in line with the XRD results, the highly dispersion state of W and Mo on the ZrO_2 surface. Additionally, any absorption bands attributable to d-d transitions has not been identified (for $600 < \lambda < 750$ nm [45,46]) in all the UV-vis spectra indicating that M^{6+}

are the main form of molybdenum and tungsten species. By contrast, both Ce^{3+} and Ce^{4+} forms coexist at the catalysts surface.

3. 4. Acidic performance of aerogel nanostructured catalysts

The surface acidity of catalyst plays an important role toward the SCR activity, since the NH_3 adsorption on the acidic sites is one of the most critical steps in the NO-SCR process. It has been verified that the SCR catalysts were progressively deactivated and even finally completely deactivated due to the disappearance of acid sites [47]. The NH_3-TPD experiments were performed in order to explore the total acidity and strength of surface acidic sites of aerogel catalysts. The recorded NH_3-TPD curves are illustrated in Fig. 4. The most intense and broad peaks with a maximum at ~ 200 °C, 380 °C and 530 °C, registered between 100 and 600 °C in the NH_3-TPD profile of the pure zirconia, are associated with the ammonia desorbed species from various acid sites, with different strengths and thermal stabilities (weak, medium and strong). In fact, it is recognized that the NH_3 desorption from weak, medium and strong acidic sites occur in the 180-250, 260-330 and 340-500 °C temperatures ranges, respectively [48]. As also shown in Fig 4, the addition of cerium, molybdenum and tungsten, separately (binary catalysts) or simultaneously (ternary catalysts), induces a slight decrease of the total acidity of support, especially, the medium and strong ones, perhaps due to the existence of diverse interactions between the zirconia and the supported active species (Ce↔Zr ; Mo↔Zr and /or W↔Zr) which probably cover or change the nature of some acidic sites at ZrO_2 surface. Similar observation, indicating a progressive decrease of the surface acidity of Pd/Ni-Al catalysts, after Ni addition, has been noticed by Hong et al. [49]. The authors explained this fact by the decrease in the quantity of exposed unsaturated Al^{3+} ions at the surface which induces a decrease in the number of surface acidic sites upon increasing the Ni content.

3. 5. Redox performance of aerogel nanostructured catalysts

It is believed that the surface acidity of catalyst plays a key role in the adsorption and activation of ammonia, especially at high temperature but not at low temperature, where the SCR reactivity is controlled by the redox properties of catalyst [50]. Herein, the H_2-TPR analyses were done to investigate the redox behavior of catalysts. The obtained H_2-TPR profiles are displayed in Fig. 5.

As shown in Fig. 5, no H_2 consumption peaks are recorded for the pure ZrO_2 indicating that Zr^{4+} is a non-reducible cation in the investigated temperature range [51,52]. In fact, it was reported that pure zirconia does not show any reduction peak below 900 °C [53]. In the contrary to catalytic support, two peaks with low intensity are detected at around 380 and 567 °C in the H_2-TPR profile of the binary CeO_2-ZrO_2 and can be ascribed to the reduction of the surface oxygen and cerium species (from Ce^{4+} to Ce^{3+}), respectively [24,25,54]. Two H_2 consumption peaks are detected also in the case of the aerogel MoO_3- ZrO_2; the first one at 409 °C can be linked to the reduction of both surface oxygen species and octahedral molybdenum groups (with different degrees of polymerization and weakly bounded to support) from M^{6+} to Mo^{4+} [55,56]. The second one at 725 °C corresponds to the second reduction step of polymeric octahedral Mo species (from Mo^{4+} to Mo^0) and first reduction step of the isolated tetrahedral Mo^{6+} species (in strong interactions with the support) [55,56]. Similar peaks are detected at 446 °C and 730 °C in the H_2-TPR profile of the CeO_2-MoO_3-ZrO_2 sample. Noting that the higher area and intensity of the first peak, if compared to that characterizing MoO_3-ZrO_2, could indicate the reduction of more higher quantity of surface oxygen, cerium and/or M^{6+} octahedral ploymolybdates species present on the CeO_2-MoO_3-ZrO_2 surface. This can suggest the existence of strong interactions between Ce and Mo which most probably contribute to (i) improve the dispersion degree of polymolybdates and cerium

species, and (ii) increase the concentration, mobility and reducibility of surface oxygen species which would be beneficial for the low temperature SCR activity. Better redox property of CeO_x/MoO_3-TiO_2 than that of $CeMo_{0.5}O_x$ has been observed also by Geng et al. [57] and has been correlated with the interactivity between Ce and Mo. A peak, which cannot be clearly observed because of the final temperature of the experiments, seems to start at around 600 °C in the H_2-TPR profile of WO_3-ZrO_2 and might represent the reduction of W species (W^{6+}) [9,17,58-62]. The CeO_2-WO_3-ZrO_2 ternary sample displays a different reduction behaviour if compared to corresponding binary (WO_3-ZrO_2) since a new H_2 consumption peaks are observed between 400 and 800 °C on the TPR profile of ternary catalyst and could be accredited to the reduction of surface oxygen, cerium and different type of tungsten species [16,17,24,58-62]. It is worth mentioning that the easier reduction of W species in the presence of cerium may be due to a good dispersion of these species certainly induced by a synergistic interaction among the different elements (oxygen, W and Ce). Similar result has been obtained by Song et al. [16] for CWZ catalysts. The authors reported that the reduction temperature peak of surface CeO_2 moved to higher values, and that of WO_3 shifted toward lower temperature due to the strong synergetic interaction between CeO_2 and WO_3.

3. 6. Catalytic behaviour

The NO-SCR activities of new ZrO_2, CeO_2-ZrO_2, MoO_3-ZrO_2, WO_3-ZrO_2, MoO_3-CeO_2-ZrO_2 and WO_3-CeO_2-ZrO_2 aerogel catalysts were evaluated under a fixed relatively high GHSV (120 000 h^{-1}), with 3.5 % H_2O. The NO conversion as a function of temperature, are exposed in Fig. 6.

It is clearly seen from Fig. 6 that, the zirconia support and the binary catalysts (CeO_2-ZrO_2, MoO_3-ZrO_2 and WO_3-ZrO_2) exhibit rather poor SCR activity at a temperature ranging from 150 to 500 °C. In fact, the maximum NO conversion into N_2 reached around 12 % (at 500 °C), 18 % (at 500 °C), 35 % (at 440 °C) and 50 % (at 500 °C) over ZrO_2, WO_3-ZrO_2, CeO_2-ZrO_2, and MoO_3-ZrO_2 samples, respectively. This is could reveal the low SCR reactivity of acid sites of the pure zirconia, on one hand, and the acidic and redox sites, generated by the addition of a single additive M (M = Ce, Mo or W), on the other hand. Noticeably, the DeNOx activities of ternary systems are significant higher than those of corresponding binary in the whole temperature range (150-500 °C). Therefore, the T 50 and T 90 (temperatures for which 50 % and 90 % of NO conversion into N_2 are achieved, respectively) are: 310 and 400 °C for WO_3-CeO_2-ZrO_2; 285 and 350 °C for MoO_3-CeO_2-ZrO_2. If we compare, in term of conversion and selectivity, these two latter catalysts towards temperature (Table 4), the addition of molybdenum leads to more efficient ternary aerogel catalyst which help to reduce a maxmium of 99 % NO into essentially N_2 (98 %) at 450 °C.

The better catalytic performance of ternary aerogel catalysts with respect to corresponding binary can be principally associated with the synergetic effect of W-Ce and, particularly, Mo-Ce strong interactions which seems to play a crucial role in improving the concentration and mobility of surface oxygen species, enhancing the reactivity of acidic and redox sites and, consequently, increasing the NO-SCR activity of solids. Similar results, demonstrating that the co-existence of MoO_3 and CeO_2-ZrO_2 is very important for the promotion of the SCR activity, has been already obtained by Z. Liu et al. [24]. The authors concluded that the doped Mo on CeO_2-ZrO_2 could donate electron to the adjacent Ce^{4+}, resulting in the synergetic effect between Mo and Ce which can effectively promote the redox property of MoO_3/CeO_2-ZrO_2 catalyst and contribute to enhance the NH_3-SCR activity. Furthermore, Ding et al. [23] stated that the mobility of oxygen at the $CeMo_{0.5}Z_2O_x$ catalyst surface was greatly improved due to the strong synergetic effect among Zr, Ce and Mo species. Their results indicate that the stronger oxidation reduction ability of $CeMo_{0.5}Z_2O_x$

benefits the excellent SCR reaction performance. On the other hand, Li et al. [9] affirmed that the higher surface area, the strongest synergistic interaction between different elements, the superior redox property and the highly dispersed or amorphous WO_3 species contributed to the excellent SCR activity of the CeO_2-ZrO_2-WO_3 catalyst.

A comparative study of NO-SCR results, obtained with our new MoO_3-CeO_2-ZrO_2 and WO_3-CeO_2-ZrO_2 aerogel catalysts and those reported in the literature using comparable systems [3,17,23,24], prepared by different methods (Table 5), points out a high catalytic performances of our new systems, especially at high temperatures (> 400 °C), under relatively higher GHSV (120000 h^{-1}).

4. Conclusion and perspectives

The fundamental research presented in this paper demonstrates the successful synthesis of new series of nanostructured and mesoporous aerogel catalysts (CeO_2-ZrO_2, MoO_3-ZrO_2, WO_3-ZrO_2, MoO_3-CeO_2-ZrO_2 and WO_3-CeO_2-ZrO_2) for the NO-SCR by NH_3 process. XRD and N_2-physisorption studies showed that all the samples calcined at 500 °C display a good cristallinity of the tetragonal phase of ZrO_2 (as the major or only phase detected), developed mesoporous texture ($S_{BET} \geq 130$ m^2/g and $V_{PT} > 0.37$ cm^3/g) and nanometer size (in the range of 6.6-10.6 nm). The presence of oxygen species, acidic and redox sites on the catalysts surface was proved using the H_2-TPR and NH_3-TPD experiments. Moreover, the highly dispersion state of Ce, Mo and W species on the surface of binary and ternary catalysts was verified through the XRD and UV-vis analysis. In the NO-SCR reaction, which was performed between 150 and 500 °C, at relatively high GHSV (120 000 h^{-1}), in the presence of excess oxygen and water, it was revealed that the MoO_3-CeO_2-ZrO_2 and WO_3-CeO_2-ZrO_2 ternary catalysts exhibit much better activity than that of corresponding binary, in the whole temperature range. The synergetic Ce↔Mo and Ce ↔W interactions, are suggested to be responsible for the substantial improvement of the SCR activity of ternary samples. MoO_3-CeO_2-ZrO_2 was found to be the most active catalyst in this reaction with: a maximum of 99 % NO conversion into essentially N_2 (98 %) at 450 °C and more than 90 % NO conversions with a high N_2 selectivity (≥ 97 %) between 350 and 500 °C.

Futher studies are in progress to examine the stabililty and hydrothermal stability of the new MoO_3-CeO_2-ZrO_2 and WO_3-CeO_2-ZrO_2 SCR catalysts, to evaluate their resistance under H_2O and SO_2, to probe, via new tehniques, the nature of actives sites at their surface and thus identify the type of the SCR reaction mecanisme.

Acknowledgements

The authors wish to express their sincere thanks to Thomas Cacciaguerra for XRD analysis. The Franco-Tunisian Cooperation (French Institute of Tunisia, SSHN grant) and Laboratory of Chemistry of Materials and Catalysis (LCMC) of Tunisia are gratefully acknowledged for the Financial support.

References

[1] X. Yu, F. Cao, X. Zhu, X, Zhu, X. Gao, Z. Luo, K. Cen, Selective catalytic reduction of NO over Cu-Mn/OMC Catalysts: Effect of preparation method, Aerosol and Air Qual. Res. 17 (2017) 302-313.
[2] W. Shan, F. Liu, H. He, X. Shi, C. Zhang, A superior Ce-W-Ti mixed oxide catalyst for the selective catalytic reduction of NO_x with NH_3, Appl. Catal. B: Environ. 115-116 (2012) 100-106.
[3] Z. Song, P. Ning, Q. Zhang , H. Li, J. Zhang, Y. Wang, X. Liu, Z. Huang, Activity and hydrothermal stability of CeO_2–ZrO_2–WO_3 for the selective catalytic reduction of NO_x with NH_3, J. Environm. Sci. 42 (2016) 168-177.
[4] W. Shan, F. Liu, Y. Yu, H. He, The use of ceria for the Selective Catalytic Reduction of NOx with NH_3. Chin. J. Catal. 35 (2014) 1251-1259.
[5] D. H. Shang, W. Cai, W. Zhao, Y. F. Bu, Q. Zhong, Catalytic Oxidation of NO to NO_2 Over Co-Ce-Zr Solid Solutions: Enhanced Performance of Ce-Zr Solid Solution by Co, Catal. Lett. 144 (2014) 538-544.
[6] Y. Zeng, K.-G. Haw, Y. Wang, S. Zhang, Z. Wang, Q. Zhong, S. Kawi, Recent progress of CeO_2-TiO_2 based catalysts for selective catalytic reduction of NOx by NH_3, ChemCatalChem (2020) https://doi.org/10.1002/cctc.202001307.
[7] W. Shan, Y. Yu, Y. Zhang, G. He, Y. Peng, J. Li, H. He, Theory and practice of metal oxide catalyst design for the selective catalytic reduction of NOx with NH_3, Catal. Today (2020) https://doi.org/10.1016/j.cattod.2020.05.015.
[8] C. E. Hori, H. Permana, K. Y. S. Ng, A. Brenner, K. More, K. M. Rahmoeller, D. Belton, Thermal stability of oxygen storage properties in a mixed CeO_2-ZrO_2 system, Appl. Catal. B 16 (1998) 105-117
[9] J. Li, Z. Song, P. Ning, Q. Zhang, X. Liu, H. Li, Z. Huang, Influence of calcination temperature on selective catalytic reduction of NOx with NH_3 over CeO_2-ZrO_2-WO_3 catalyst J. Rare Earths, 33 (2015) 726-735.
[10] W. Shan, F. Liu, H. He, X. Shi, C. Zhang, Novel cerium–tungsten mixed oxide catalyst for the selective catalytic reduction of NOx with NH_3, Chem. Commun. 47 (2011) 8046-8048.
[11] W. Shan, F. Liu, Y. Yu, H. He, C. Deng, X. Zi, High-efficiency reduction of NO_x emission from diesel exhaust using a $CeWO_x$ catalyst, Catal. Commun. 59 (2015) 226- 228.
[12] N. K. Liu, Y. Huo, Z. Yan, W Shan, H. He, Inhibitory role of excessive NH_3 in NH_3-SCR on CeWOx at low temperatures, Catal. Sci. Technol. (2020) https://doi.org/10.1039/D0CY00096E
[13] H. D. Xu, Q. L. Zhang, C. T. Qiu, T. Lin, M. C. Gong, Y. Q. Chen, Tungsten modified MnOx-CeO_2/ZrO_2 monolith catalysts for selective catalytic reduction of NOx with ammonia. Chem. Eng. Sci. 76 (2012) 120-128.
[14] H. D. Xu, Y. Wang, Y. Cao, Z. T. Fang, T. Lin, M.C. Gong, Y.Q. Chen, Catalytic performance of acidic zirconium-based composite oxides monolithic catalyst on selective catalytic reduction of NOx with NH_3, Chem. Eng. J. 240 (2014) 62-73
[15] Y. Li, H. Cheng, D. Li, Y. Qin, Y. Xie, S. Wang, WO_3/CeO_2-ZrO_2, a Promising Catalyst for Selective Catalytic Reduction (SCR) of NOx with NH_3 in Diesel Exhaust. Chem. Commun. 17 (2008) 1470-1472.
[16] Z. Song, Q. Zhang , J. Zhang, P. Ning, H. Li, Y. Wang, M. Wang, Y. Duan, Effet of WO_3 content on the catalytic activity of CeO_2-ZrO_2-WO_3 for selective catalytic reduction of NO with NH_3, J. Fuel Chem Technol, 43 (2015) 701-707
[17] P. Ning, Z. Song, H. Li, Q. Zhang, X. Liu, J. Zhang, X. Tang, Z. Huang, Selective catalytic reduction of NO with NH_3 over CeO_2–ZrO_2–WO_3 catalysts prepared by different methods, Appl. Surf. Sci. 332 (2015) 130-137.

[18] J. Liu, X. Shi, Y. Shan, Z. Yan, W. Shan, Y. Yu, H. He, Hydrothermal Stability of CeO_2-WO_3-ZrO_2 Mixed Oxides for Selective Catalytic Reduction of NOx by NH_3, Environ. Sci. Technol. 52 (2018) 11769−11777.
[19] Y. Jiang, Z. Xing, X. Wang, S. Huang, Q. Liu, J. Yang, MoO_3 modified CeO_2/TiO_2 catalyst prepared by a single step sol-gel method for selective catalytic reduction of NO with NH_3, J. Ind. Eng. Chem. 29 (2015) 43-47.
[20] Y. Jiang, X. Wang, Z. Xing, C. Bao, G. Liang, Preparation and Characterization of CeO_2- MoO_3/TiO_2 Catalysts for Selective Catalytic Reduction of NO with NH_3, Aerosol Air Qual. Res. 17 (2017) 2726-2734.
[21] Y. Jiang, M. Lu, S. Liu, C. Bao, G. Liang, C. Lai, W. Shia, S ; Ma, Deactivation by HCl of CeO_2–MoO_3/TiO_2 catalyst for selective catalytic reduction of NO with NH_3, RSC Adv. 8 (2018) 17677-16684 .
[22] L. Li, P. Li, W. Tan, K. Ma, W. Zou, C. Tang, L. Dong, Enhanced low-temperature NH_3-SCR performance of CeTiOx catalyst via surface Mo modification, Chinese J. Catal. 41 (2020) 364-373.
[23] S. Ding, F. Liu, X. Shi, K. Liu, Z. Lian, L. Xie, H. He, Significant Promotion Effect of Mo Additive on Novel Ce-Zr Mixed Oxide Catalyst for the Selective Catalytic Reduction of NO, ACS Appl. Mater. Interfaces 7 (2015) 9497-9506.
[24] Z. Liu, H. Su, J. Li, Y. Li, Novel MoO_3/CeO_2-ZrO_2 catalyst for the selective catalytic reduction of NOx by NH_3, Catal. Commun. 65 (2015) 51-54.
[25] J. Arfaoui, A. Ghorbel, C. Petitto, G. Delahay, Novel V_2O_5-CeO_2-TiO_2-SO_4^{2-} nanostructured aerogel catalyst for the low temperature selective catalytic reduction of NO by NH_3 in excess O_2, Appl. Catal. B: Environ. 224 (2018) 264-275.
[26] S. Mathur, M. Arya, R. Jain, S. K. Sharma, Effect of Annealing Temperature on Structural, Electrical and Optical Properties of TiO2 Nanopowder, J Nanostruct. 7 (2017) 121-126 Spring.
[27] C. Liu, J. W. Shi, C. Gao, C. Niu, Manganese oxide-based catalysts for low-temperature selective catalytic reduction of NO x with NH_3: A review, Appl. Catal. A: Gen. 522 (2016) 54-69.
[28] M. Fernández-García, A. Martínez-Arias, J. C. Hanson, J. A. Rodriguez, Nanostructured Oxides in Chemistry: Characterization and Properties, Chem. Rev. 104 (2004) 4063-4104.
[29] S. Gao, X. Chen, H. Wang, J. Mo, Z Wu, Y. Liu, X. Weng, Ceria supported on sulphated zirconia catalyst for selective catalytic reduction of NO with NH_3, J. Colloid Interface Sci. 394 (2013) 515-521.
[30] R. C. Gravie, Stabilization of the tetragonal structure in zirconia microcrystals, J. Phys. Chem 82 (1978) 218-224.
[31] W. Khaodee, N. Tangchupong, B. Jongsomjit, P. Praserthdam, S. Assabumrungrat, A study on isosynthesis via CO hydrogenation over ZrO2–CeO2 mixed oxide catalysts, Catal. Commun. 10 (2009) 494-501.
[32] M. Kang, T. H. Yeon, E. D. Park, J. E. Yie, J. M. Kim , Novel MnO_x Catalysts for NO Reduction at Low Temperature with Ammonia, Catal. Lett. 106 (2006) 77-80. [33] M. Thommes, K. Kaneko, A. V. Neimark, J. P. Olivier, F. Rodriguez-Reinoso, J. Rouquerol, K. S. W. Sing, Physisorption of gases, with special reference to the evaluation of surface area and pore size distribution (IUPAC Technical Report), Pure Appl. Chem. 87 (2015) 1051–1069.
[34] M. A. López-Mendoza, R. Nava, C. Peza-Ledesma, B. Millán-Malo, R. Huirache-Acuña, P. Skewes, E.M. Rivera-Muñoz, Characterization and catalytic performance of Co-Mo-W sulfide catalysts supported on SBA-15 and SBA-16 mechanically mixed, Catal. Today 271 (2016) 114-126.

[35] V. Morozova, T. V. Khamova, I. G. Polyakova, Effect of Precursors on the Preparation and Texture of Mesoporous γ-Al_2O_3 Powders, Inorg. Mater. 56 (2020) 353–359.
[36] Z. Guerra-Que, G. Torres-Torres, H. Pérez-Vidal, I. Cuauhtémoc-Lopez, A. Espinosa de los Monteros, J. N. Beltramini, D. M. Frias-M´arquez, Silver nanoparticles supported on zirconia–ceria for the catalytic wet air oxidation of methyl tert-butyl ether. RSC Adv. 7 (2017) 3599-3610.
[37] R. Ismail, J. Arfaoui, Z. Ksibi, A. Ghorbel, G. Delahay, Effect of the iron amount on the physicochemical properties of Fe-ZrO_2 aerogel catalysts for the total oxidation of toluene in the presence of water vapor. J. Porous Mat. 27 (2020) 1847-1852.
[38] R. Huirache-Acuña, B. Pawelec, E. Rivera-Muñoz, R. Nava, J. Espino, J.L.G. Fierro, Comparison of the morphology and HDS activity of ternary Co-Mo-W catalysts supported on P-modified SBA-15 and SBA-16 substrates, Appl. Catal. B : Environm. 92 (2009) 168-184.
[39] R. Huirache-Acuña, B. Pawelec, E. M. Rivera-Muñoz, R. Guil López, J.L.G. Fierro, Characterization and HDS activity of sulfided CoMoW/SBA-16 catalysts: Effects of P addition and Mo/(Mo +W) ratio, Fuel 198 (2017) 145-158.
[40] T. I. Bhuiyan, P. Arudra, M. N. Akhtar, A. M. Aitani, R. H. Abudawoud, M.A. Al-Yami, S. S. Al-Khattaf, Metathesis of 2-butene to propylene over W-mesoporous molecular sieves: A comparative study between tungsten containing MCM-41 and SBA-15, Appl. Catal. A : Gen. 467 (2013) 224-234.
[41] X. L. Yang, W. L. Dai, R. Gao, H. Chen, H. Li, Y. Cao, K. Fan, Synthesis, characterization and catalytic application of mesoporous W-MCM-48 for the selective oxidation of cyclopentene to glutaraldehyde, J. Mol. Catal A : Chem. 241 (2005) 205-214 .
[42] Y. Miao, G. Lu, X. Liu, Y. Guo, Y. Wang, Y. Guo, Effects of preparation procedure in sol-gel method on performance of MoO_3/SiO_2 catalyst for liquid phase epoxidation of propylene with cumene hydroperoxide, J. Mol. Catal. A: Chem. 306 (2009) 17-22.
[43] P. Yuan, C. Cui, W. Han, X. Bao, The preparation of Mo/γ-Al_2O_3 catalysts with controllable size and morphology via adjusting the metal-support interaction and their hydrodesulfurization performance, Appl. Catal. A: Gen. 524 (2016) 115-125.
[44] M. Rada, M. Zagrai, S. Rada, A. Bot, E. Culea, Effects on the characteristics of bonding and local structure in molybdenum-lead-lead dioxide glasses and vitroceramics, J. Alloys Compd. 705 (2017) 327-332.
[45] C. Zhan, F. Chen, H. Dai, J. Yang, M. Zhong, Photocatalytic activity of sulfated Modoped TiO_2@fumed SiO2 composite: A mesoporous structure for methyl orange degradation, Chem. Eng. J. 225 (2013) 695-703.
[46] F. Adam, A. Iqbal, Silica supported amorphous molybdenum catalysts prepared via solgel method and its catalytic activity, Micropor. Mesopor Mat. 141 (2011) 119-127.
[47] H. Xu, S. Liu, Y. Wang, Q. Lin, C. Lin, L. Lan, Q. Wang, Y. Chen, Promotional effect of Al_2O_3 on WO_3/CeO_2-ZrO_2 monolithic catalyst for selective catalytic reduction of nitrogen oxides with ammonia after hydrothermal aging treatment, Appl. Surf. Sci. 427 (2018) 656-669.
[48] Z. Song, Y. Xing, T. Zhang, J. Zhao, J. Wang, Y. Mao, B. Zhao, X. Zhang, M. Zhao, Z. Ma, Effectively promoted catalytic activity by adjusting calcination temperature of Ce-Fe-Ox catalyst for NH_3-SCR, Appl Organometal Chem. (2019) e5446. https://doi.org/10.1002/aoc.5446
[49] E. Hong, S-A. Jeon, S-S. Lee, C-H. Shin, Methane combustion over Pd/Ni-Al oxide catalysts: Effect of Ni/Al ratio in the Ni-Al oxide support, Korean J. Chem. Eng. 35 (2018) 1815-1822.
[50] P. Forzatti, Present status and perspectives in de-NOx SCR catalysis, Appl. Catal. A: Gen. 222 (2001) 221-236.

[51] S. N. Basahel, M. Mokthar, E. H. Alsharaeh, T. T. Ali, H. A. Mahmoud, K. Narasimharao, Physico-Chemical and Catalytic Properties of Mesoporous CuOZrO2 Catalysts, Catalysts 6 (2016) 57-77.
[52] R. Ismail, J. Arfaoui, Z. Ksibi, A. Ghorbel, G. Delahay, Ag/ZrO2 and Ag/Fe–ZrO2 catalysts for the low temperature total oxidation of toluene in the presence of water vapor, Transit Met Chem. Transit Met Chem 45 (2020) 501-509.
[53] H. S. Roh, W.S. Dong, K.W. Jun, S.E. Park, Partial Oxidation of Methane over Ni Catalysts Supported on Ce-ZrO2 Mixed Oxide, Catal. Lett. 30 (2001) 88-89.
[54] Z. Liu, S. Zhang, J. Li, J. Zhu, L. Ma, Novel V2O5-CeO2/TiO2 catalyst with low vanadium loading for the selective catalytic reduction of NOx by NH3, Appl. Catal. B: Environ. 158-159 (2014) 11-19.
[55] Y. Jiang, X. Zhang, M. Lu, C. Bao, G. Liang, C. Lai, W. Shi, S. Ma, Activity and characterization of Ce–Mo–Ti mixed oxide catalysts prepared by a homogeneous precipitation method for selective catalytic reduction of NO with NH3, J. Taiwan Inst. Chem. Eng. 86 (2018) 133-140.
[56] J. Arfaoui, A. Ghorbel, C. Petitto, G. Delahay, A new V2O5-MoO3-TiO2-SO4 2- nanostructured aerogel catalyst for Diesel DeNOx technology. New J Chem 44 (2020) 16119-16134.
[57] Y. Geng, X. Chen, S. Yang, F. Liu, W. Shan, Promotional Effects of Ti on a CeO2-MoO3 Catalyst for the Selective Catalytic Reduction of NOx with NH3, ACS Appl. Mater. Interfaces 9 (2017) 16951-16958
[58] Y. Peng, J. H. Li, L. Chen, J. H. Chen, J. Han, H. Zhang, W. Han, Alkali metal poisoning of a CeO2-WO3 catalyst used in the selective catalytic reduction of NOx with NH3: an experimental and theoretical study, Environ. Sci. Technol. 46 (2012) 2864-2869.
[59] Z. R. Ma, D. Weng, X. D. Wu, Z. C. Si, Effect of WOx modification on the activity, adsorption and redox properties of CeO2 catalyst for NOx reduction with ammonia. J. Environ. Sci. 24 (2012) 1305-1316.
[60] Z. Song, L. Yin, Q. Zhang, P. Ning, Y. Duan, J. Wang, X. Liu, K. Long, Z. Huang, Relationship between the WO3 states and reaction pathway over CeO2-ZrO2-WO3 catalysts for selective catalytic reduction of NO with NH3, Mol. Catal 437 (2017) 95-104.
[61] L. Chen, D. Weng, J. Wang, D. Weng, L. Cao, Low- temperature activity and mechanism of WO3- modified CeO2- TiO2 catalyst under NH3- NO/NO2 SCR conditions, Chinese J. Catal. 39 (2018) 1804-1813.
[62] R. Fan, Z. Li, Y. Wang, C. Zhang, Y. Wang, Z. Ding, X. Guoab, R. Wang, Effects of WO3 and SiO2 doping on CeO2–TiO2 catalysts for selective catalytic reduction of NO with ammonia, RSC Adv. 10 (2020) 5845-5842.

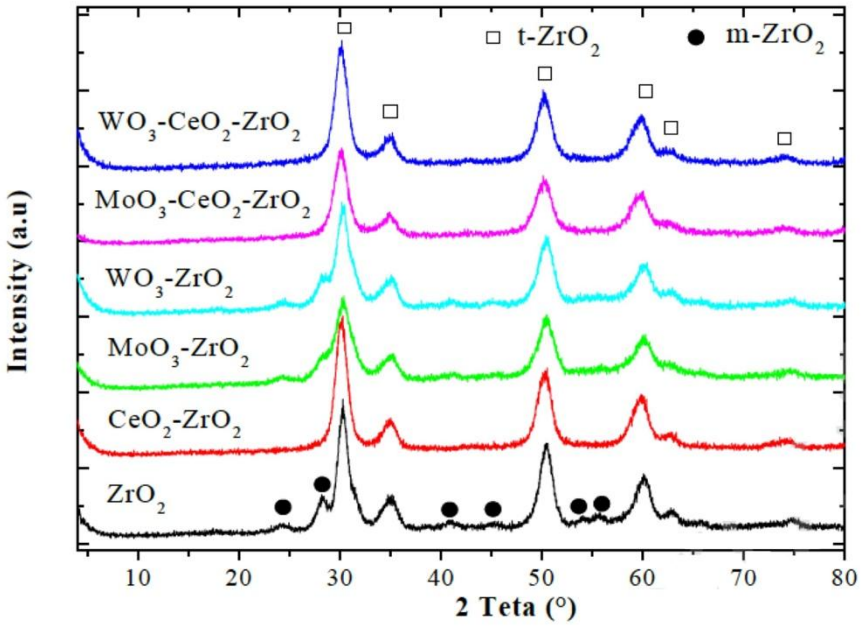

Figure 1. XRD patterns of nanostructured mesoporous aerogel catalysts.

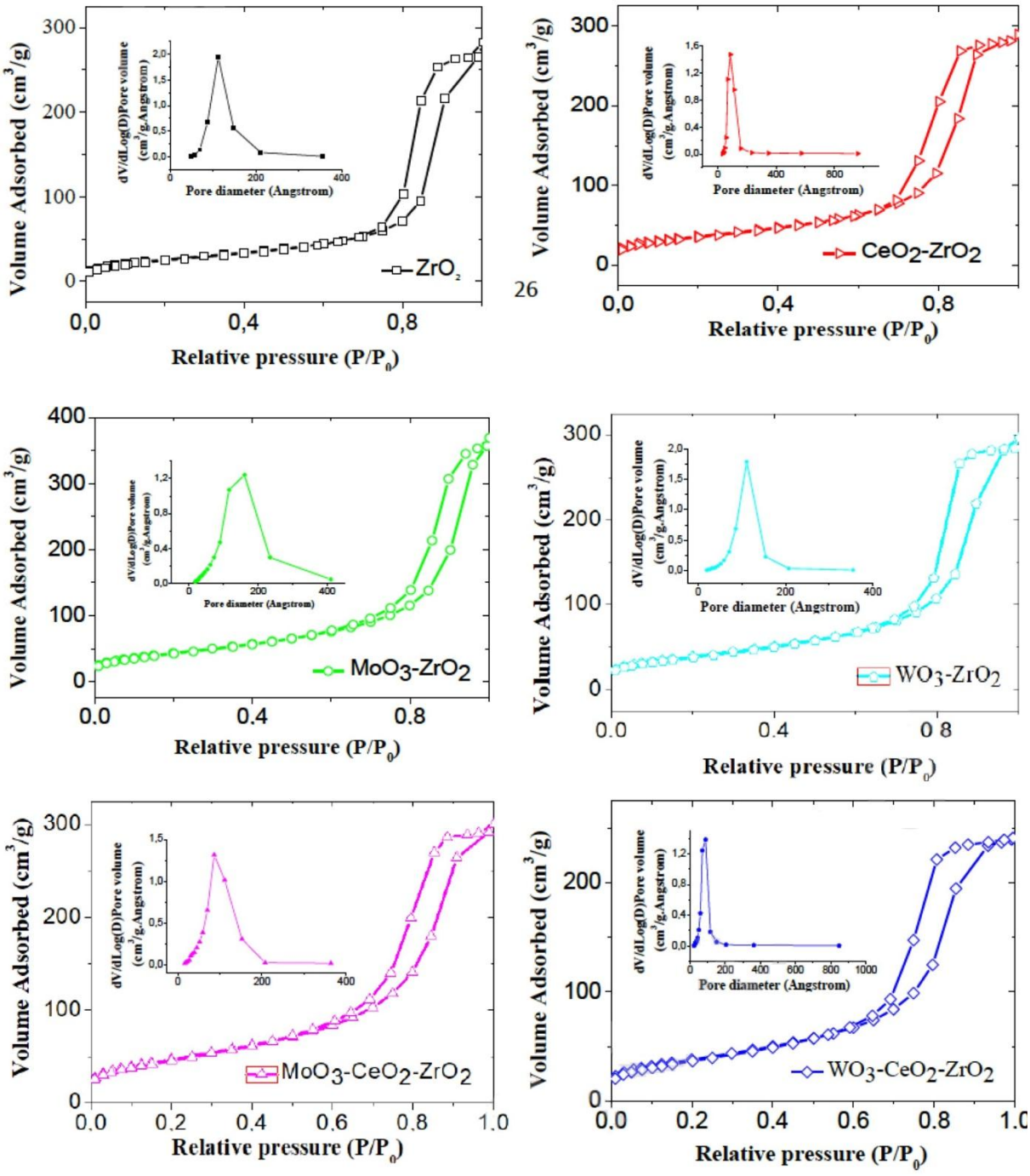

Figure 2. N_2-adsorption-desorption isotherms and corresponding pore size distribution curves of nanostructured mesoporous aerogel catalysts.

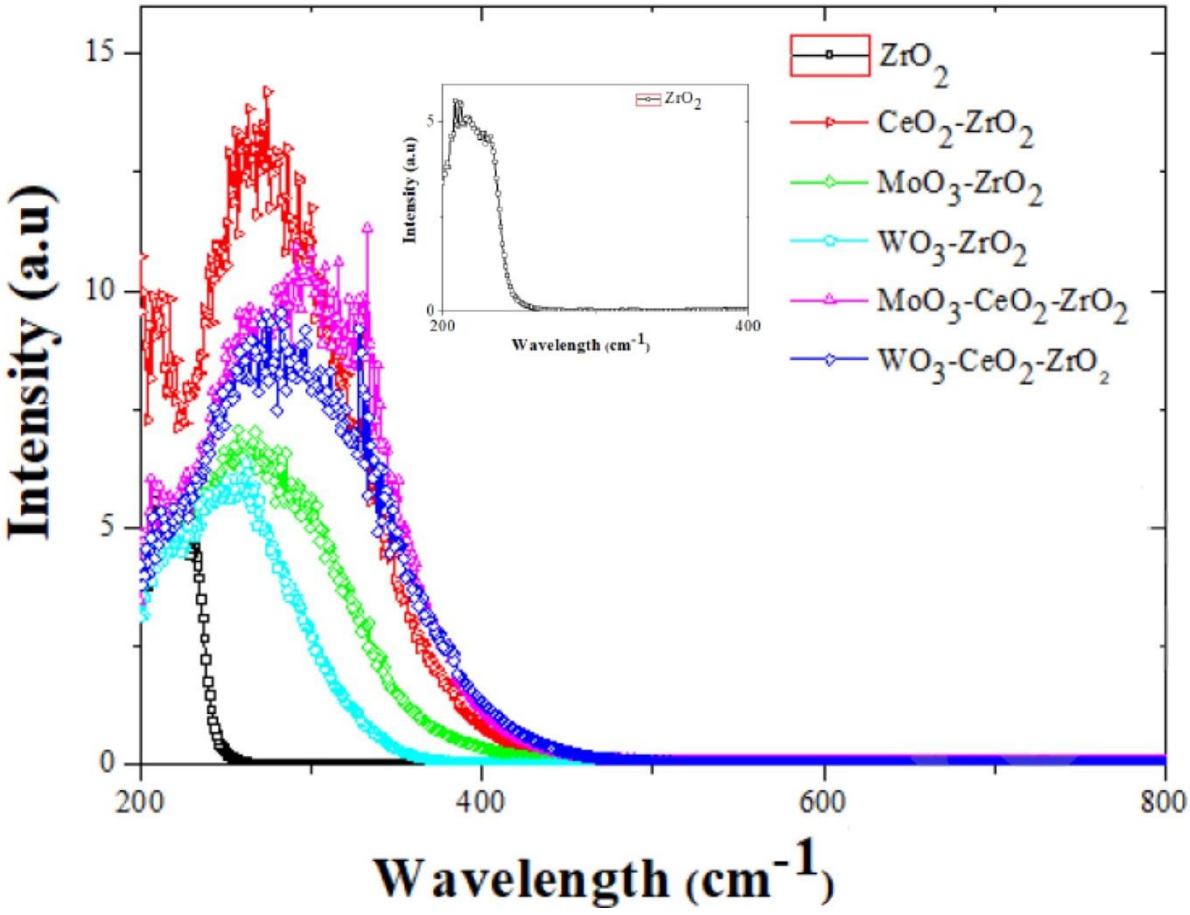

Figure 3. DRUV-Vis spectra of nanostructured mesoporous aerogel catalysts.

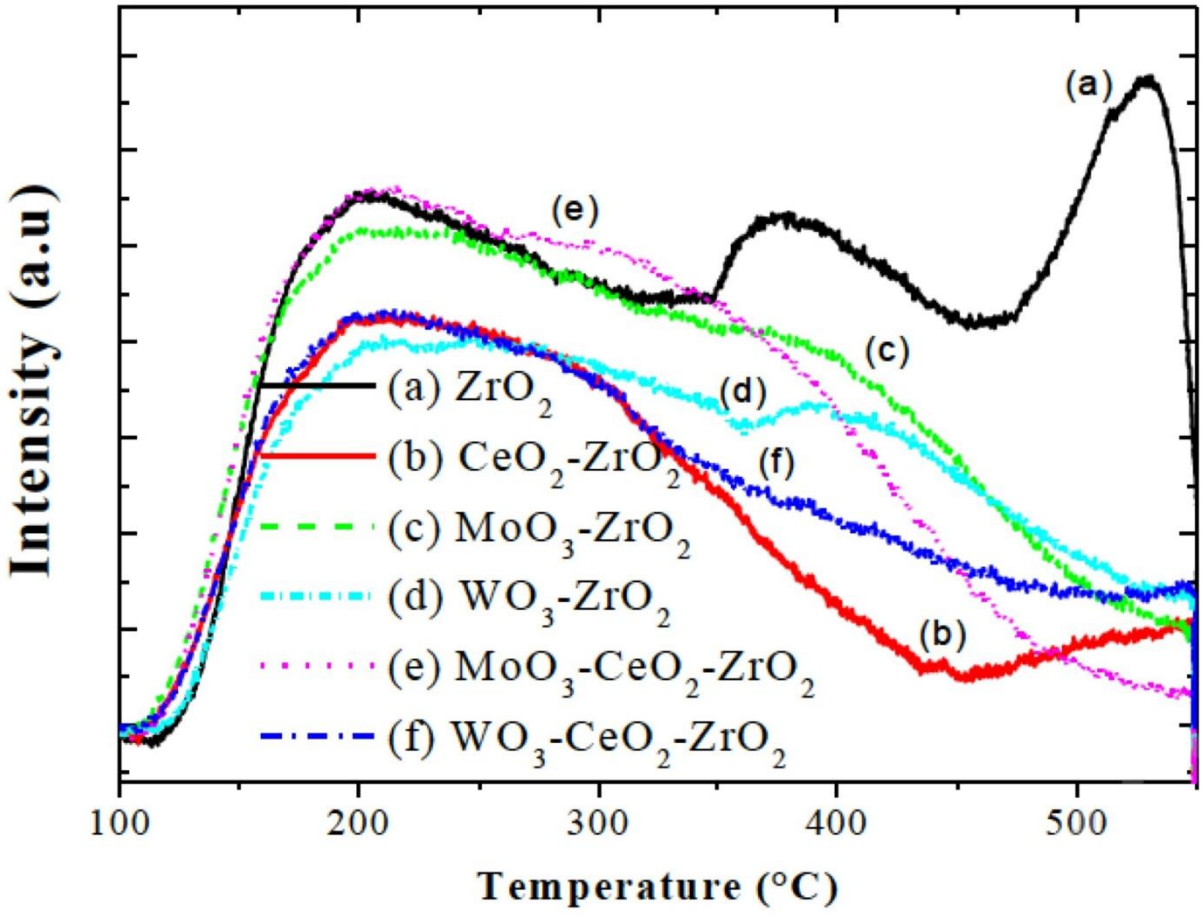

Figure 4. NH_3-TPD profiles of nanostructured mesoporous aerogel catalysts.

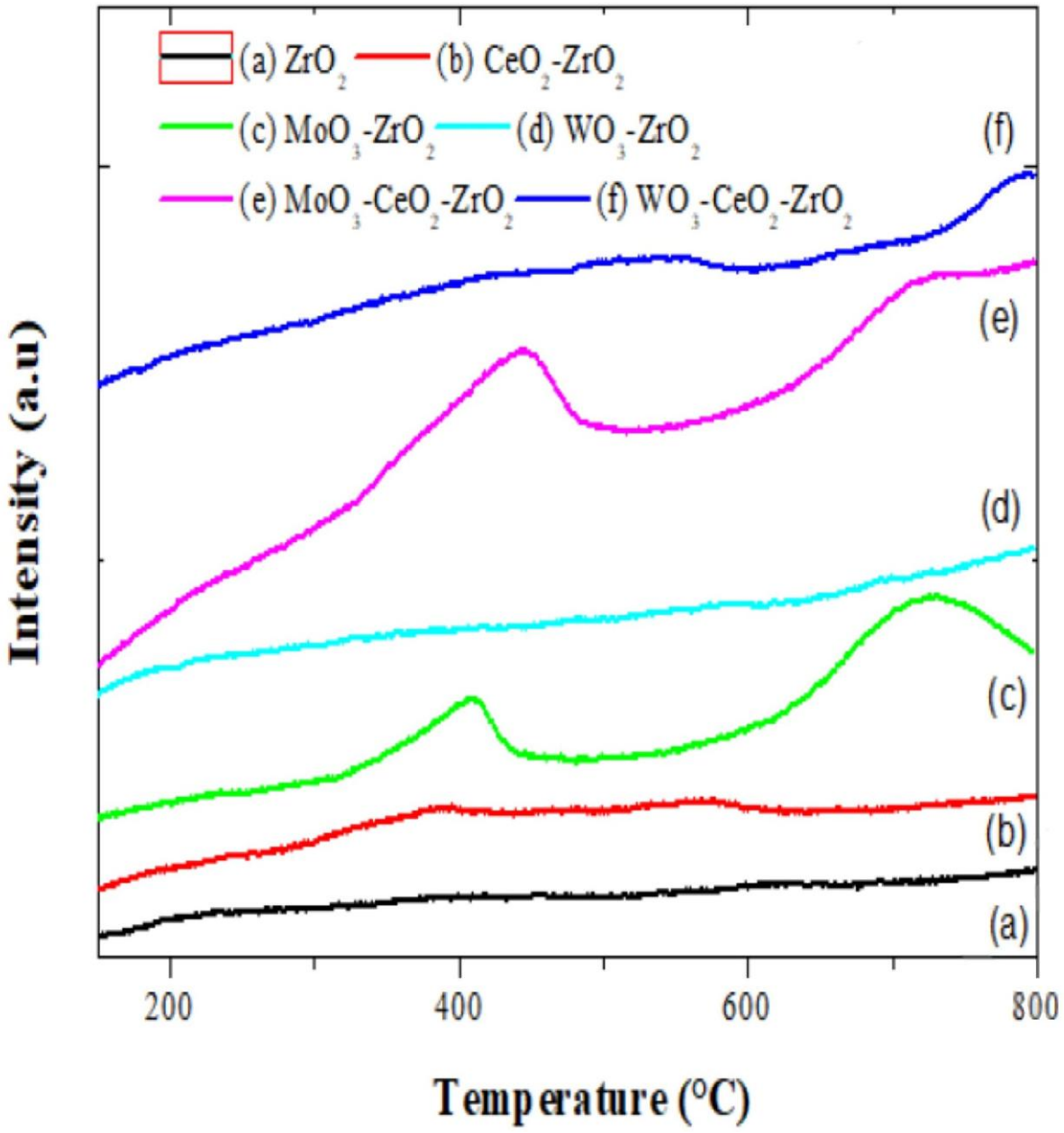

Figure 5. H_2-TPR profiles of nanostructured mesoporous aerogel catalysts

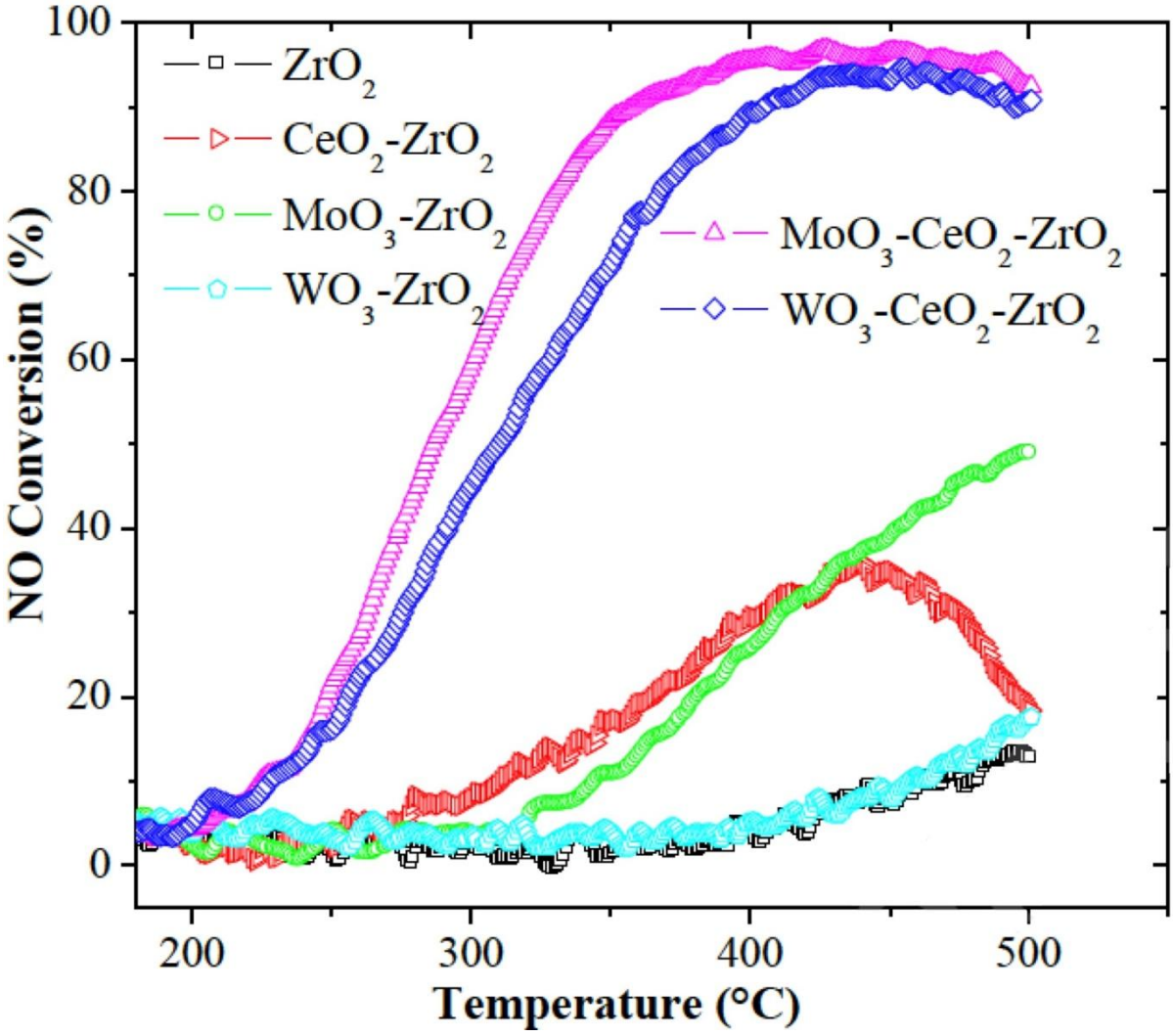

Figure 6. NO conversion versus reaction temperature over the nanostructured mesoporous aerogel catalysts.

Table 1. XRD phases and ZrO_2 crystallites size of nanostructured mesoporous aerogel catalysts.

Aerogel catalysts	XRD phases	FWHM (°)	ZrO_2 crystallites size D (nm)
ZrO_2	t-ZrO_2 (Maj) + m-ZrO_2 (Min)	1.245	10.6
CeO_2- ZrO_2	t-ZrO_2	1.386	9.5
MoO_3- ZrO_2	t-ZrO_2 (Maj) + m-ZrO_2 (Min)	2.004	6.6
WO_3- ZrO_2	t-ZrO_2 (Maj) + m-ZrO_2 (Min)	1.632	8.1
MoO_3-CeO_2- ZrO_2	t-ZrO_2	1.590	8.3
WO_3-CeO_2- ZrO_2	t-ZrO_2	1.498	8.8

Table 2. Textural properties of nanostructured mesoporous aerogel catalysts.

Aerogel catalysts	BET surface area (m^2/g)	Total pore volume (cm^3/g)	Average Pore diameter (Φ_{pore}, Å)
ZrO_2	93	0.41	111
CeO_2- ZrO_2	130	0.45	91
MoO_3- ZrO_2	155	0.55	109
WO_3- ZrO_2	136	0.44	96
MoO_3-CeO_2- ZrO_2	168	0.45	79
WO_3-CeO_2- ZrO_2	135	0.37	77

Table 3. UV-vis diffuse reflectance band positions and assignments found in the literature for M transition metals (M = W and Mo).

Species	DRUV-vis band position: λ (nm)	Type of transition	Assignments	Ref.
W	210-270	$O^{2-} \rightarrow W^{6+}$ LMCT	Isolated tetrahedral W^{6+}	[34,38-41]
	263	$O^{2-} \rightarrow W^{6+}$ LMCT	Oligomerized tungustate species	[40]
	300-375	$O^{2-} \rightarrow W^{6+}$ LMCT	Polymeric octahedral W^{6+}	[34,38-41]
	430-450	-	Crystalline WO_3	[41]
Mo	200-270	$O^{2-} \rightarrow Mo^{6+}$ LMCT	Isolated tetrahedral Mo^{6+}	[34, 38,39,42,43]
	260-280 300-350	$O^{2-} \rightarrow Mo^{6+}$ LMCT	Polymeric octahedral Mo^{6+}	[34, 38, 39, 42,43]
	290-300	Mo-O-Mo	Oligomerized molybdate species	[34,42]
	360-385	$O^{2-} \rightarrow Mo^{5+}$ LMCT	-	[44]
	> 320	-	Crystalline MoO_3	[42]
	600-750	d-d transition	Molybdenum (V)	[45,46]

Table 4. Catalytic behaviour of MoO_3-CeO_2-ZrO_2 and WO_3- CeO_2-ZrO_2 nanostructured mesoporous aerogel catalysts calcined at 500 °C in NO-SCR by NH_3: [NO] = [NH_3] = 0.10 %, [O_2] = 8.00 % balance with He (GHSV) = 120 000 h^{-1} with 3.5 % H_2O.

Aerogel catalyst	Temperature (°C)	NO Conversion (%)	Selectivity (%)		
			N_2	N_2O	NO_2
MoO_3- CeO_2-ZrO_2	200	5	100	0	0
	250	21	100	0	0
	300	57	100	0	0
	350	90	99	1	0
	400	96	98.5	1.5	0
	450	99	98	2	0
	500	93	97	3	0
WO_3- CeO_2-ZrO_2	200	5	100	0	0
	250	16	95	5	0
	300	45	92	8	0
	350	71	91	9	0
	400	90	97	3	0
	450	93	> 99	< 1	0
	500	90	98	2	0

Table 5. Comparative study of the NO-SCR activity over various MoCeZr and WCeZr catalysts.

Catalysts	Preparation method	SCR test conditions	Results	Ref.
MoO_3-CeO_2-ZrO_2 (Aerogel)	Sol-Gel supercritical drying	[NO] = [NH_3] = 0.10 % [O_2] = 8.00 % GHSV = 120 000 h^{-1} 3.5 % H_2O m_{Cat} = 0.05 g	Above 90 % NO conversion in 350-500 °C N_2 selectivité ≥ 97 %	This work
MoO_3/CeO_2- ZrO_2	Hydrothermal Impregnation	[NO] = [NH_3] = 0.05 % [O_2] = 5.00 % GHSV = 98 000 h^{-1} m_{Cat} = 0.12 g	Above 90 % NO conversion in 250-400 °C	[24]
$CeMo_{0.5}$-Zr_2O_x	Homogenous precipitation	[NO] = [NH_3] = 0.05 % [O_2] = 5.00 % GHSV = 50 000 h^{-1} m_{Cat} = 0.75 g	100 % NO conversion in 250-400 °C N_2 selectivité > 80 %	[23]
WO_3-CeO_2-ZrO_2 (Aerogel)	Sol-Gel supercritical drying	[NO] = [NH_3] = 0.1 % [O_2] = 8.00 % GHSV = 120 000 h^{-1} 3.5 % H_2O m_{Cat} = 0.05 g	Above 90 % NO conversion in 400-500 °C N_2 selectivité ≥ 97 %	This work
CeO_2-ZrO_2-WO_3 (CZW)	Hydrothermal	[NO] = [NH_3] = 0.06 % [O_2] = 5.00 % GHSV = 60 000 h^{-1} V_{Cat} = 0.4 mL	Above 90 % NO conversion in 201-495 °C N_2 selectivité > 91 %	[3]
CeO_2-ZrO_2-WO_3	*Hydrothermal (The best)* Imprenation	[NO] = [NH_3] = 0.06 % [O_2] = 5.00 % GHSV = 60 000 h^{-1}	Above 90 % NO Conversion in 195-450 °C	[17]
	Co-precipitation Sol gel: xerogel	V_{Cat} = 1 mL	[N_2O] < 12 ppm	